Detection of cervical lesions by multivariate analysis of diffuse reflectance spectra: a clinical study

Vasumathi Gopala Prabitha, Sambasivan Suchetha, Jayaraj Lalitha Jayanthi, Kamalasanan Vijayakumary Baiju, Prabhakaran Rema, et al.
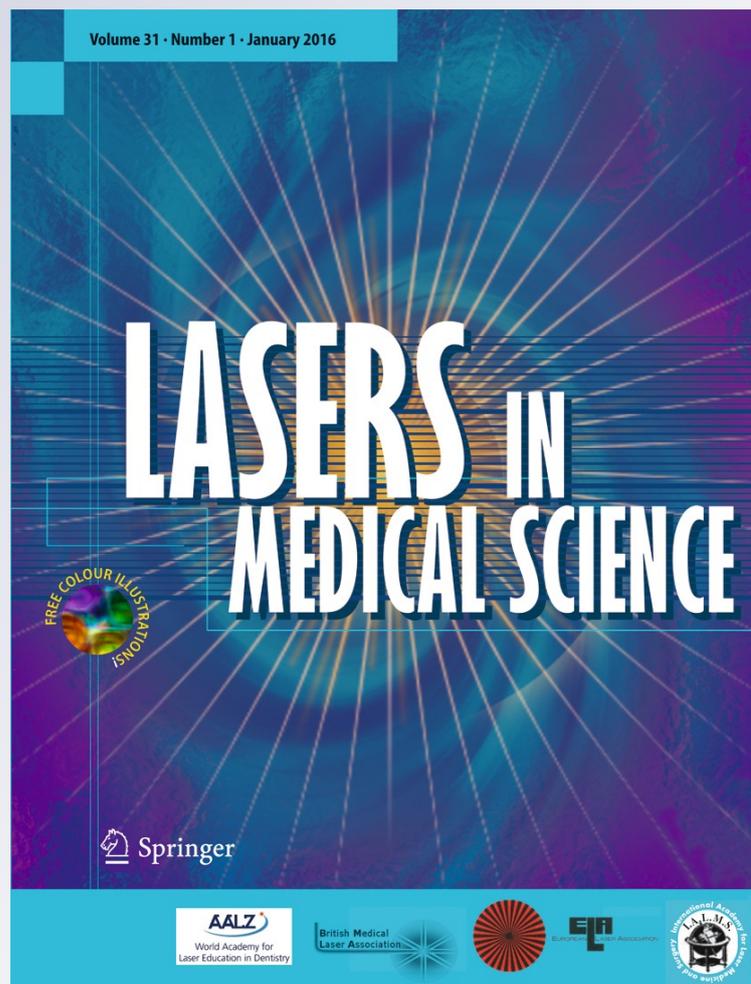
Volume 31 · Number 1 · January 2016

FREE COLOUR ILLUSTRATIONS!

LASERS IN MEDICAL SCIENCE

Springer

Springer

Springer

CrossMark

ORIGINAL ARTICLE

Detection of cervical lesions by multivariate analysis of diffuse reflectance spectra: a clinical study

Vasumathi Gopala Prabitha[1] · Sambasivan Suchetha[2] · Jayaraj Lalitha Jayanthi[2] ·
Kamalasanan Vijayakumary Baiju[3] · Prabhakaran Rema[2] · Koyippurath Anuraj[1] ·
Anita Mathews[2] · Paul Sebastian[2] · Narayanan Subhash[1,4]

Abstract Diffuse reflectance (DR) spectroscopy is a non-invasive, real-time, and cost-effective tool for early detection of malignant changes in squamous epithelial tissues. The present study aims to evaluate the diagnostic power of diffuse reflectance spectroscopy for non-invasive discrimination of cervical lesions in vivo. A clinical trial was carried out on 48 sites in 34 patients by recording DR spectra using a point-monitoring device with white light illumination. The acquired data were analyzed and classified using multivariate statistical analysis based on principal component analysis (PCA) and linear discriminant analysis (LDA). Diagnostic accuracies were validated using random number generators. The receiver operating characteristic (ROC) curves were plotted for evaluating the discriminating power of the proposed statistical technique. An algorithm was developed and used to classify non-diseased (normal) from diseased sites (abnormal) with a sensitivity of 72 % and specificity of 87 %. While low-grade squamous intraepithelial lesion (LSIL) could be discriminated from normal with a sensitivity of 56 % and specificity of 80 %, and high-grade squamous intraepithelial lesion (HSIL) from normal with a sensitivity of 89 % and specificity of 97 %, LSIL could be discriminated from HSIL with 100 % sensitivity and specificity. The areas under the ROC curves were 0.993 (95 % confidence interval (CI) 0.0 to 1) and 1 (95 % CI 1) for the discrimination of HSIL from normal and HSIL from LSIL, respectively. The results of the study show that DR spectroscopy could be used along with multivariate analytical techniques as a non-invasive technique to monitor cervical disease status in real time.

Keywords Diffuse reflectance spectroscopy · Principal component analysis · Linear discriminant analysis · Multivariate analysis · Cervical cancer detection · Optical biopsy

Introduction

Cervical cancer represents a significant and growing concern worldwide due to its high prevalence, and more than 85 % of this global burden occurs in developing countries [1]. In India, it ranks as the first most frequent cancer among women [2]. About 95 % of cervical cancers contain the high-risk human papillomavirus (HPV), HPV-16 [3]. The interval between the acquisition of HPV infection and invasive cancer usually takes many years, and this provides a great opportunity to detect precancerous lesions during its early stages. The conventional screening is based on Papanicolaou (Pap) smear test followed by colposcopy and biopsy. Implementation of effective screening by Pap smear has resulted in decreased incidence of cervical cancers in Western countries. Nonetheless, there is no effective screening program being implemented in India for early detection of cervical cancers. Cytology results are inherently prone to sample-quality variation, subjective interpretation error, and false-negative results. Colposcopy is expensive and highly subjective, as its accuracy depends on the training and experience of the colposcopist [4–6]. Patients

✉ Narayanan Subhash
subhashnarayanan@gmail.com

1 Biophotonics Laboratory, Centre for Earth Science Studies, Akkulam, Thiruvananthapuram 695 031, Kerala, India

2 Regional Cancer Centre, Medical College P.O., Thiruvananthapuram 695 011, Kerala, India

3 Department of Statistics, Government College for Women, Thiruvananthapuram 695014, Kerala, India

4 Sascan Meditech Pvt Ltd., CIME, BMS College of Engineering, Basavanagudi, Bull Temple Road, Bangalore 560019, India

may be required to make multiple visits for colposcopic assessment, getting histopathology results, and then for follow-up treatment. Thus, providing all services in a single visit is essential for the success of cervical cancer screening in low-resource communities.

The significant cost of vaccines and political or logistical barriers could delay implementation of HPV vaccines in many developing countries [7]. Even though visual inspection with acetic acid (VIA) may have advantages of low cost and minimal infrastructure, it is subjective in nature. These current strategies can be improved by developing cost-effective, non-invasive, and objective screening tools using optical technologies. These optical technologies have the ability to visualize tissue structure and metabolism at the sub-cellular level in real-time for the early detection of cervical lesions [8, 9].

Diffuse reflectance spectroscopy (DRS), also known as elastic scattering spectroscopy (ESS), is an optical spectroscopic technique that has shown great potential for non-invasive and real-time detection of oral cancer [10–12], ovarian cancer [13], cervical cancer [8, 14–16], breast cancer [17], bladder cancer [18], and esophageal cancer [19]. When the light travels through tissue, it undergoes single or multiple scattering by the cellular and extracellular constituents having different refractive indices and gets attenuated due to absorption by the chromophores. After multiple elastic scattering and absorption, some of the incident light returns back at random angles to the surface of the tissue, which is known as diffusely reflected light. This light contains information about the absorption and reduced scattering coefficients of tissue and hence carries evidence on the concentration of different chromophores, nuclear size, morphology, and structure of the scatterers or components, such as lipid membrane and collagen fibers, present in tissue. In comparison, light scattering spectroscopy (LSS) that records singly backscattered light provides morphologic information about the number and size distribution of nuclei in the epithelial cell layer and allows us to study changes in nuclear morphologic features that are well-established histopathologic hallmarks of precancerous and cancerous changes [8].

During neoplastic progression, biochemical and morphological changes in tissue lead to changes in the characteristics of the diffusely reflected light. As precancers develop, cervical tissues are characterized by increase in chromatin concentration, nuclear size and shape, nuclear to cytoplasmic ratio, and metabolic activity. Dellas et al. have shown that microvessel density, which is proportional to vascular volume, increases during cervical precancer development [20].

Mirabel et al. noted that reflectance spectroscopy could distinguish columnar normal epithelium from high-grade dysplasia with higher specificity as compared to fluorescence detection [14]. Multimodal techniques involving tissue fluorescence and DRS were utilized to obtain a better understanding of the relationship between spectroscopic measurements and morphology in freshly excised cervical tissues [21]. A combination of diffuse reflectance and fluorescence spectroscopy suggested that the two techniques provide complementary diagnostic information for detection of oral and cervical precancers [15, 22]. Georgakoudi et al. developed a technology called trimodal spectroscopy (TMS), combining intrinsic fluorescence, diffuse reflectance, and light scattering spectroscopy for analyzing cervical squamous intraepithelial lesions (SILs) with good diagnostic accuracies [8]. In vivo confocal imaging provides high-resolution cervical images for the detection of dysplasia [23]. Although screening strategies like multispectral imaging [24], confocal microscopy, and optical coherence tomography [25] benefit women in the industrialized countries, they may not be cost-effective for widespread application in the third-world countries. In light of this, a simple, real-time, objective, and affordable screening test using diffuse reflectance spectroscopy would provide a reliable and effective means for reducing the burden of cervical cancer in developing countries.

The present clinical study aims to develop a multivariate statistical algorithm for the discrimination of abnormal cervical lesions from normal by principal component analysis (PCA) and linear discriminant analysis (LDA) of white light-illuminated DR spectra recorded with a point-monitoring fiber-optic probe. The discrimination ability of the algorithm developed was analyzed using receiver operating characteristic (ROC) curves, and the results are presented.

Materials and methods

Study population and lesion grouping

The study population consisted of 48 cervical sites in 34 patients (average age of 40 ± 10 years) with abnormal Pap smear, recruited from the outpatient (OP) clinic of the Regional Cancer Centre (RCC), Thiruvananthapuram. The study was approved by the Ethical Committee of RCC, Vide HEC no. 28/2011 of January 12, 2012. Participants were required to sign an informed consent indicating their willingness to participate in the study. The trial was registered at the Clinical Trial Registry India (CTRI) under no. CTRI/2014/02/004424.

The patients recruited for the study were examined by a gynaecologist, and suspicious cervical lesions identified visually were spectroscopically probed using the DR point-monitoring system. After recording spectral data of all the identified sites in a patient, punch biopsy was taken from all these sites for histological examination. Based on the histopathological report, the sampled sites were classified as normal (14 sites), squamous metaplasia (16 sites), koilocytic atypia (7 sites), cervical intraepithelial neoplasia (CIN) 1 (2 sites) and CIN 3 (6 sites), and carcinoma in situ (CIS) (3 sites). Since the sample sizes for CIN 1 and CIS were

limited, the analysis was performed by grouping the lesions into three categories, viz., normal, low-grade squamous intraepithelial lesion (LSIL), and high-grade squamous intraepithelial lesion (HSIL). Histopathologically normal squamous epithelium, inflammatory tissues, and squamous metaplasia, which is the physiological replacement of the endocervical columnar epithelium by newly formed squamous epithelium, are grouped under normal category. Koilocytic atypia and CIN 1 were grouped under LSIL (9 cases); CIN 3 and CIS were grouped as HSIL (9 cases); and for easy representation, LSIL-HSIL categories were further grouped together as diseased or abnormal (Table 1).

Point-monitoring system

The schematic of the DR system [12] used for point monitoring of cervical tissues is shown in Fig. 1. It consists of a tungsten halogen lamp (Ocean Optics, USA; model LS-1-LL) for tissue illumination and a miniature fiber-optic spectrometer (Ocean Optics, USA; model USB 2000FL VIS-NIR) connected to the USB port of a laptop computer for recording of diffusely reflected white light spectra. The fiber-optic probe used for point monitoring of cervix had a central fiber for illumination and six surrounding fibers (each fiber has a core diameter of 400 μm) for collection of DR light, with the fibers encased in a stainless steel (SS) ferule of 6 mm diameter and 15 mm length. The center-to-center distance between the illumination and collection fibers was 500 μm at the probe tip. A disposable PVC sleeve was inserted at the probe tip to avoid stray light from entering the spectrometer and for providing extra hygiene. An optimal spacer separation of 3 mm was maintained with the help of this PVC sleeve between the tissue surface to probe tip that provided maximum overlap between the excitation and collection areas. Before placing the probe in gentle contact with the cervix, it was disinfected by dipping in Cidex solution (2.45 %w/v glutaraldehyde) for 20 min and rinsed with distilled water and dried with sterile cotton. After completion of spectral recordings, the PVC sleeve that was in contact with the tissue was removed using tweezers and disposed off. The probe and tweezers were then
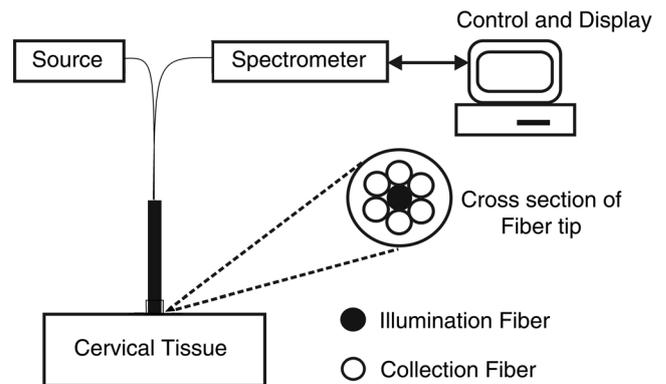

Fig. 1 Schematic of diffuse reflectance (DR) point-monitoring system

sterilized by dipping in the Cidex solution and kept aside for the next set of measurements.

Data acquisition

The DR spectra were recorded in the 450–750-nm wavelength range with a boxcar width of 10 nm for 40 scans and integration time of 100 ms. The background spectrum was recorded prior to measurements without turning the halogen lamp on, and the OOI Base32 software was configured to automatically subtract the same from the recorded spectrum to eliminate the effects of ambient light. A set of eight DR measurements were taken from each site, and the mean spectra for each site were determined for further analysis. The average spectra were normalized with respect to the maximum intensity to minimize inter-patient variation.

Statistical procedure

As a first step, we simplified the classification by dividing the obtained data into normal and abnormal. PCA was performed on the above data sets for dimension reduction, followed by LDA to distinguish normal cervical tissues from abnormal [26]. Diagnostic accuracies, such as sensitivity (Se), specificity (Sp), positive predictive value (PPV), and negative predictive value (NPV), were determined from the discriminant function scatterplot with cutoff as the weighted average of the centroids of the selected groups. The validation of

Table 1 Grouping of histopathologic categories

Histopathologic category	No. of sites	Clinical category	Groups	No. of sites
Normal	14	Normal	Normal	30
Squamous metaplasia	16			
Koilocytic atypia	7	LSIL	Abnormal	18
CIN 1	2			
CIN 3	6	HSIL		
Carcinoma in situ	3			

LSIL low-grade squamous intraepithelial lesion, *HSIL* high-grade squamous intraepithelial lesion, *CIN* cervical intraepithelial neoplasia

diagnostic accuracies was done using a subset of a moderately large sample size (70 %) of the patients from each group, which were randomly selected using random number generators in Microsoft Excel functions. For such 70 different trial sets of samples in each lesion pair, the developed multivariate diagnostic algorithm was applied to calculate the diagnostic accuracies. The arithmetic mean and standard error (AM±SE) of diagnostic accuracies were calculated for each lesion pair and tabulated.

ROC curves were plotted using discriminant function scores for evaluating the performance of DR-based diagnostic algorithms for the screening of cervical lesions. Area under the curve (AUC) quantifies the performance of DRS for differentiating normal cervical sites from abnormal. Since the abnormal group consisted of LSIL and HSIL, the same steps of the above proposed diagnostic algorithm were applied for differentiating LSIL, HSIL, and normal as pairs. For each pair, separate PCA components were calculated, following which the LDA is performed to calculate the discriminant scores to separate pairs of distinct groups. All statistical analysis was conducted using the statistical software SPSS version 16.0 for Windows.

Results

Discrimination of abnormal from normal

Figure 2 shows typical normalized DR spectra recorded from normal, LSIL, and HSIL. Marked variation was observed in the normalized spectral signatures of normal and abnormal sites in the spectral region of 450–650 nm. PCA using
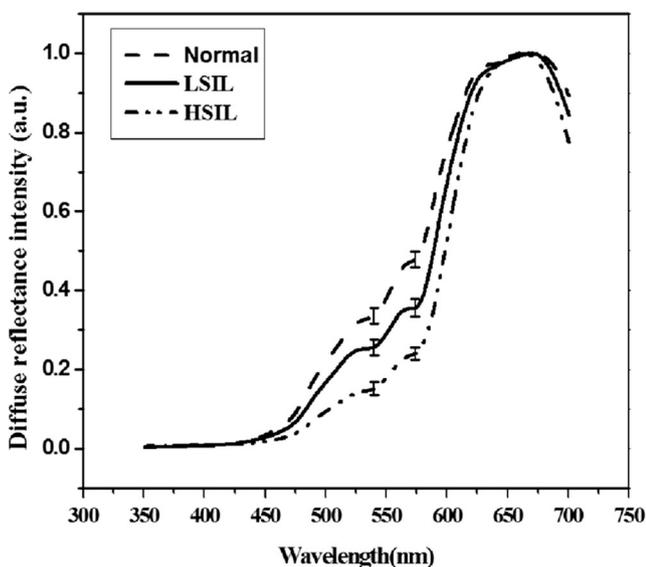

Fig. 2 Typical diffuse reflectance spectra for cervical lesions—normal, low-grade squamous intraepithelial lesion (LSIL), and high-grade squamous intraepithelial lesion (HSIL) normalized to their maximum intensities

Varimax rotation was employed on the normalized spectral data. The first seven principal components (PCs) that account for 99.82 % of the original spectral variations were used as input variables of LDA for classifying the groups as normal and abnormal by generating a discriminant function. Figure 3a shows the scatterplot for classification of normal from abnormal with the cutoff line drawn at −0.1765, the weighted average of the centroids of the selected groups. Out of the 30 histopathologically normal sites, 4 cases were misclassified as abnormal, whereas out of 18 abnormal cases, 5 were misclassified as normal. The sensitivity and specificity for discrimination between normal and abnormal were found to be 72 and 87 %, respectively. Positive and negative predictive values were 76 and 84 %, respectively.
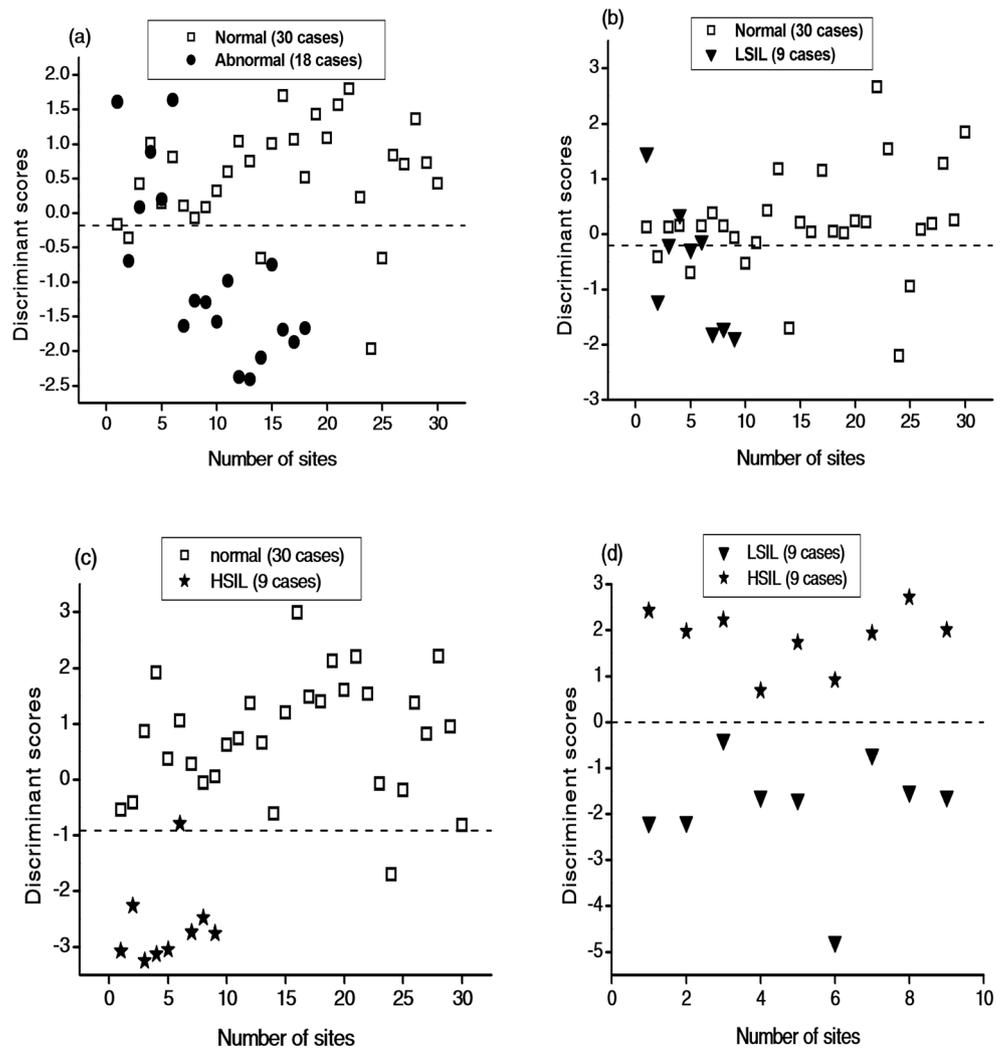
Discrimination of normal from LSIL and HSIL

The abnormal group consisting of LSIL (9 sites) and HSIL (9 sites) were classified independently with respect to normal using the same algorithm, taking all PCs into consideration. Figure 3b–d shows the scatterplots for differentiating LSIL from normal, HSIL from normal, and HSIL from LSIL, with cutoff values of −0.207, −0.9145, and 0.0, respectively.

Table 2 shows the diagnostic accuracies for differentiating various paired groups. Albeit the small sample size, we observed 100 % sensitivity and specificity for discriminating HSIL from LSIL. However, HSIL sites were discriminated from normal with 89 % sensitivity and 97 % specificity, while LSIL could be discriminated from normal with a sensitivity of 56 % and specificity of 80 %. As can be seen from Table 2, the negative predictive values for discriminating all the above pairs are high while the positive predictive values are also significant except for differentiating normal from LSIL. The arithmetic mean and standard errors of the diagnostic parameters for the validation set using repeated random selection method are also given in Table 2. In this table, the sensitivity and specificity of the validation set are 70±1.4 and 85±1.3 %, respectively, for normal and abnormal groups, while these are 54±1.9 and 79±1.1 % for normal and LSIL groups, 87±1.3 and 95±1.9 % for normal and HSIL groups, and 99±1.7 and 98±1.3 % for LSIL and HSIL groups. After reducing the discrimination bias, the validation set values are close to the training set but a shade lower in comparison for all the different groups studied. The low standard errors indicate that the mean values in the validation set are consistent estimates.

ROC analysis

ROC curves were plotted using discriminant function scores for evaluating the performance of the DR-based diagnostic algorithms. ROC curve plotted for discriminating normal from abnormal lesions yielded an AUC of 0.81 (95 % confidence interval (CI) 0.660 to 0.963) as shown in Fig. 4a. The AUC

Fig. 3 Discriminant function scatterplot of the following different lesion pairs: **a** normal-abnormal, **b** normal-LSIL, **c** normal-HSIL, and **d** LSIL-HSIL. The *dashed line* drawn at the weighted average of the centroids of data represents the cutoff value in each pair

quantifies the performance of DRS for differentiating normal cervical sites from abnormal. ROC analysis yields AUCs of 0.993 (95 % CI 0 to 1) and 1 (95 % CI 1) for discrimination of the HSIL from normal, and the HSIL from LSIL, respectively, and 0.719 (95 % CI 0.504 to 0.933) for differentiating the LSIL from normal (Fig. 4b–d).

Discussion

The metaplastic transformation in cervix provides an environment ripe for the initiation of dysplastic changes. Metaplasia itself is not a premalignant condition, and inflammation is clinically considered as non-diseased. Therefore, squamous

Table 2 Diagnostic accuracies of different cervical lesion pairs

Tissue types	Training set				Validation set (AM±SE)			
	Se (%)	Sp (%)	PPV (%)	NPV (%)	Se (%)	Sp (%)	PPV (%)	NPV (%)
Normal (30) and abnormal (18)	72	87	76	84	70±1.4	85±1.3	76±0.9	82±2.1
Normal (30) and LSIL (9)	56	80	45	86	54±1.9	79±1.1	44±1.0	84±0.9
Normal (30) and HSIL (9)	89	97	89	97	87±1.3	95±1.9	87±1.5	94±2.0
LSIL (9) and HSIL (9)	100	100	100	100	99±1.7	98±1.3	98±1.8	98±1.8

The value given in parenthesis in column 1 is the number of samples included under each category

LSIL low-grade squamous intraepithelial lesion, *HSIL* high-grade squamous intraepithelial lesion, sensitivity (*Se*)=true positive (*TP*)/TP+false negative (*FN*), specificity (*Sp*)=true negative (*TN*)/TN+false positive (*FP*), positive predictive value (*PPV*)=TP/TP+FP, negative predictive value (*NPV*)=TN/TN+FN

Fig. 4 Receiver operator characteristic curves with diagonal reference line showing the diagnostic performance of discriminant function scores for identifying the following different lesion pairs: **a** normal-abnormal (area under the curve, AUC= 0.81), **b** normal-LSIL (AUC= 0.719), **c** normal-HSIL (AUC= 0.993), and **d** LSIL-HSIL (AUC= 1)
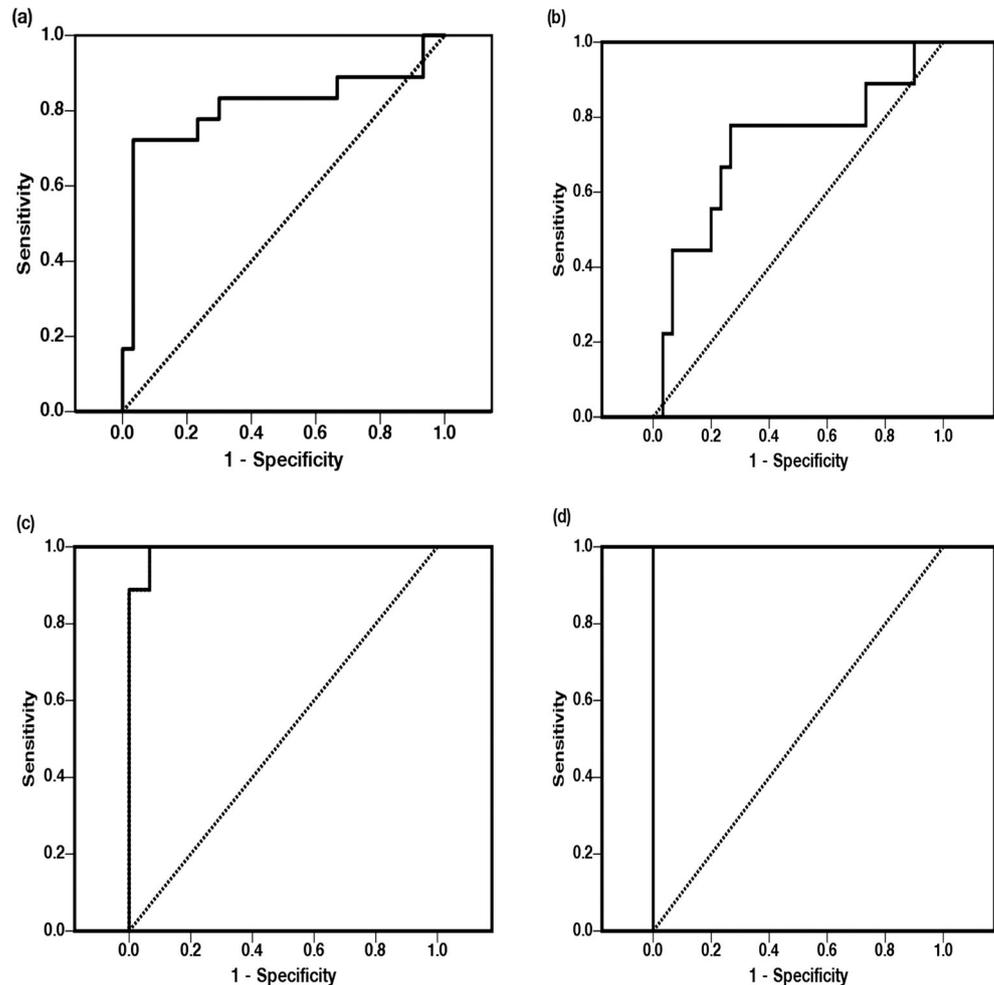
metaplasia, inflammation, and the benign changes of the cervix were grouped under normal category. Koilocytosis is a condition in which the cell has a little halo around its nucleus, which signifies the infection of the cell with HPV. Changes associated with HPV infection and CIN 1 were grouped together as LSIL, whereas CIN 2/3 and CIS were grouped together as HSIL. Table 1 shows grouping of different lesions with the results of histopathology into normal, LSIL, and HSIL.

The basis for detection of cervical lesions using DRS arises from differences in the spectral characteristics between normal and abnormal tissues due to changes in the epithelial and stromal layers. The primary absorbers in epithelial tissues are the oxygenated and deoxygenated hemoglobin, which along with the changes in tissue scattering modifies the diffusely reflected light. Variations in diffuse reflectance intensity, spectral patterns, absorption features, and stromal and epithelial scattering due to tissue vasculature are useful in the detection of changes to cervical tissue and in the discrimination between different grades of malignancy [27, 28]. Here, the algorithm developed using normalized DR spectral data accounts for the spectral shape variation between different

sites and patients. The absorption dips seen in the DR spectra of normal tissues at 542 and 574 nm are due the presence of oxygenated hemoglobin absorption. The reduced activity of the ferrochelatase enzyme that catalyzes the insertion of ferrous iron into protoporphyrin to form heme [29] results in lower hemoglobin production in malignant tissues and lowers the absorption intensities at 542 and 574 nm in the oxygenated hemoglobin spectra.

Since even a gentle contact of cervix with tip of the fiberoptic probe could cause tissue blanching due to the pressure exerted on the tissue, care was taken to minimize the effects by recording spectra from each site within 3–5 s. Nonetheless, previous reports show that probe contact pressure had no significant effect on fluorescence spectra measured from cervical tissues [30, 31] or on Raman spectra recorded from gastrointestinal tissues [32]. It was also reported that probe pressure could cause statistically significant alterations in diffuse reflectance spectra only above a certain threshold value of contact pressure, which again was dependent on the tissue type [33, 34]. Our clinical study consisted of eight measurements acquired within 2–3 min, with the black sleeve at the probe tip held in gentle contact with the surface of the cervix and the

hand holding the probe resting on the speculum to minimize and maintain the same amount of probe pressure on the tissue. In order to take care of possible fluctuations in the intensity of the light source used, a warm-up period of 20 min was given to stabilize the output power of the tungsten halogen lamp used for DR measurements. Furthermore, the DR spectra were normalized with respect to the maximum intensity of emission spectrum to compensate for changes, if any, in the intensity of the lamp output.

To extract diagnostic information from the DR spectra of cervical tissues, an algorithm was developed based on PCA and LDA. PCA is a widely used dimension-reduction technique, which is easy to implement and interpret [26]. LDA is subsequently performed to obtain thresholds for discriminating the different tissue classes. The most important quality of a diagnostic procedure is its ability to differentiate malignant from non-malignant tissues. In this study, we have obtained a specificity of 87 % for differentiating normal from abnormal tissues, which reduces false positives thereby reducing the number of unnecessary biopsies and treatment delay. In comparison, the most widely used method of Pap smear has 15–40 % false positive rate, which results in a large number of unnecessary colposcopies. Although the sensitivity of colposcopy is excellent (>90 %), it has poor specificity (<50 %) even in the hands of an expert and hence leads to unnecessary biopsies [35, 36]. In many developing countries, VIA is being explored as an alternative to Pap smear screening and colposcopy [37]. It has a sensitivity ranging from 67 to 79 % and specificity of 49 to 86 %. Even though VIA requires minimal infrastructure and is cost-effective, it is based on subjective visual interpretation, whereas DR is an objective technique to screen cervical malignancies.

Although both LSIL and HSIL are grouped together as diseased, LSIL needs follow-up and HSIL needs treatment. Therefore, it is important to distinguish LSIL from HSIL. Precancerous lesions could progress to invasive carcinoma if left untreated. Although the sample size was small, the present multivariate statistical algorithm was able to differentiate HSIL from LSIL with 100 % sensitivity and specificity and from normal with a sensitivity of 89 % and specificity of 97 % (Table 2). However, the sensitivity of discrimination is significantly lower and specificity significantly higher for separating LSIL from normal. The lower percentage of sensitivity (56 %) shows that LSIL could not be effectively classified from normal with the DR technique.

One of the commonly used methods for validation of the diagnostic accuracy of a classification algorithm is the leave-one-out (LOO) method of cross validation. When the size of the data set is moderate, there is a chance for bias in this method of cross validation. Thus, in order to validate the diagnostic accuracy of the present algorithm, another method has been proposed, where 70 % of the patients from each group were randomly selected using random number

generators. The developed multivariate diagnostic algorithm was applied to 70 different subsets of samples in each lesion pair, and the mean diagnostic accuracies were calculated along with its standard error so that bias in the diagnostic algorithm used in the training set could be minimized.

HSIL has high risk of developing into invasive cancer, if left untreated. Therefore, such lesions require immediate colposcopy and treatment, usually by loop electrosurgical excision procedure. Therefore, identifying high-grade squamous intraepithelial lesions from low-grade lesions is crucial for cervical cancer prevention. Even though the sample size is less, we could achieve 100 % diagnostic accuracy for differentiation between these two types of lesions. The DR screening, therefore, shows potential for lesions to be identified on a single visit to the clinic, and treatment can be administered in the same day for women with HSIL.

Our study findings are supported by similar DRS analytical reports for distinguishing different tissue types. Based on a reflectance study, Mirabel et al. have reported that squamous normal could be discriminated from high-grade squamous intraepithelial lesions with a sensitivity of 72 % and a specificity of 81 % and columnar normal from high-grade squamous intraepithelial lesions with sensitivity of 72 % and specificity of 83 % [14]. Similarly, using DRS in the detection of cervical precancer, Nordstrom et al. could discriminate normal squamous tissue and HSIL with a sensitivity of 82 % and a specificity of 67 % using a multivariate algorithm based on the Mahalanobis distance [15]. With the help of a multivariate statistical algorithm involving PCA and LDA, Jayanthi et al. reported, utilizing the absorption features of oxygenated hemoglobin, an overall sensitivity of 98.5 % and specificity of 96 % for distinguishing SCC from dysplastic oral lesions, while the sensitivity and specificity values were 100 and 95 %, respectively, for distinguishing dysplasia from hyperplasia [12].

Many groups have used diffuse reflectance and fluorescence spectra to detect precancer in the cervix. Richards-Kortum and co-workers measured fluorescence spectra of cervical tissue in vivo from 95 patients and classified high-grade dysplasia from all other cervical pathologies with sensitivity of 79 % and specificity of 78 % using a multivariate algorithm based on Bayes' theorem for discrimination [26]. Chang et al. reported a sensitivity and specificity of 83 % and 80 % per patient in an analysis for the detection of cervical precancer based on combined reflectance and fluorescence spectroscopy [16]. Using logistic regression and leave-one-out validation, Georgakoudi et al. reported that trimodal spectroscopy was able to detect SIL from non-SIL with a sensitivity and specificity of 92 and 71 %, respectively [8]. Recently, by collecting reflectance and fluorescence spectra from 43 patients with a quantitative spectroscopy probe, Mirkovic et al. have reported a "normalized" scattering parameter at 700 nm, which could distinguish HSIL from non-HSIL with sensitivity and specificity of 89 and 79 %, respectively; PPV and NPV of 48 and

97 %; and AUC of 0.84 [38]. Although our sample sizes were small, the higher sensitivity and specificity reported in Table 2 for discrimination between HSIL and LSIL point to the great potential of non-invasive DRS along with the multivariate analytical technique based on PCA plus LDA for screening of cervical precancers.

As compared to imaging techniques, point monitoring is a time-consuming process and there is a possibility for missing out potential lesions. However, the point-monitoring devices are comparatively less costly and are suited for low-resource settings. Once a robust algorithm is developed, involving a large number of patients, probing could be undertaken dividing the cervix into four quadrants with 6–10 measurements from each quadrant so that all potential lesions could be covered.

Taking advantage of the cost-effectiveness and technical feasibility of DR spectroscopy, the study results have more significance in developing countries, where cervical cancer often goes undetected because of the high cost of screening tests and the lack of trained personnel. It is proposed to extend the study to a larger sample size needed to improve the sensitivity to discriminate LSIL from normal cervical tissues and to generate a robust algorithm for discrimination of benign tumors and inflammations from premalignant lesions.

References

1. World Cancer Fact Sheet: World Cancer Burden (2008) UICC Global Cancer Control, Cancer Research UK, International Agency for Research on Cancer, World Health Organisation (WHO)

2. Human papillomavirus and related cancers, Fact Sheet 2010, India, WHO/ICO Information Centre on HPV and Cervical Cancer

3. zur Hausen H (1994) Molecular pathogenesis of cancer of the cervix and its causation by specific human papillomavirus types. Curr Top Microbiol Immunol 186:131–156

4. Buxton EJ, Luesley DM, Shafi MI et al (1991) Colposcopically directed punch biopsy; a potentially misleading investigation. Br J Obstet Gynaecol 98:1273–1276

5. Chenoy R, Manohar S, Redman CWE et al (1994) Cervical cytologic abnormalities and negative colposcopy: histologic assessment. Int J Gynecol Cancer 4:348–351

6. Massad LS, Collins YC (2003) Strength of correlations between colposcopic impression and biopsy histology. Gynecol Oncol 89: 424–428

7. Agosti JM, Goldie SJ (2007) Introducing HPV vaccine in developing countries—key challenges and issues. N Engl J Med 356:1908–1910

8. Georgakoudi I, Ellen ES, Mullar MG et al (2002) Tri-modal spectroscopy for the detection and characterization of cervical precancers in vivo. Am J Obstet Gynecol 186:374–382

9. Drezek R, Guillaud M, Collier T et al (2003) Light scattering from cervical cells throughout neoplastic progression: influence of nuclear morphology, DNA content, and chromatin texture. J Biomed Opt 8:7–16

10. Subhash N, Mathews A, Sebastian P et al (2006) Oral cancer detection using diffuse reflectance spectral ratio R540/R575 of oxygenated hemoglobin bands. J Biomed Opt 11:014018–014023

11. Mallia J, Thomas SS, Mathews A et al (2008) Oxygenated hemoglobin diffuse reflectance ratio for in vivo detection of oral precancer. J Biomed Opt 13:041306–0413015

12. Jayanthi JL, Nisha GU, Manju S et al (2011) Diffuse reflectance spectroscopy: diagnostic accuracy of a non-invasive screening technique for early detection of malignant changes in the oral cavity. BMJ open. 1–7

13. Utzinger U, Brewer M, Silva E et al (2001) Reflectance spectroscopy for in vivo characterization of ovarian tissue. Lasers Surg Med 28:56–66

14. Mirabal YN, Chang SK, Atkinson EN et al (2002) Reflectance spectroscopy for *in vivo* detection of cervical precancer. J Biomed Opt 7:587–594

15. Nordstrom RJ, Burke L, Niloff JM et al (2001) Identification of cervical intraepithelial neoplasia (CIN) using UV-excited fluorescence and diffuse-reflectance tissue spectroscopy. Lasers Surg Med 29:118–127

16. Chang SK, Mirabel YN, Atkinson EN et al (2005) Combined reflectance and fluorescence spectroscopy for *in vivo* detection of cervical pre-cancer. J Biomed Opt 10:024031–024042

17. Zhu C, Palmer GM, Breslin TM et al (2008) Diagnosis of breast cancer using fluorescence and diffuse reflectance spectroscopy: a Monte-Carlo-model–based approach. J Biomed Opt 13:034015–034030

18. Koenig F, Larne R, Enquist H et al (1998) Spectroscopic measurement of diffuse reflectance for enhanced detection of bladder carcinoma. Urology 51:342–347

19. Lovat LB, Johnson K, Mackenzie GD et al (2006) Elastic scattering spectroscopy accurately detects high grade dysplasia and cancer in Barrett's oesophagus. Gut 55:1078–1083

20. Dellas A, Moch H, Schultheiss E et al (1997) Angiogenesis in cervical neoplasia: microvessel quantitation in precancerous lesions and invasive carcinomas with clinicopathological correlations. Gynecol Oncol 67:27–33

21. Alex RZ, Oliva E, Koufman H et al (2002) Fluorescence and reflectance spectra of freshly excised cervical tissue. Proc. SPIE 4613, Optical Biopsy IV. 51

22. Richard RA, Wen G, Dania D et al (2008) Autofluorescence and diffuse reflectance spectroscopy of oral epithelial tissue using a depth-sensitive fiber-optic probe. Appl Opt 47:825–34

23. Collier T, Guillaud M, Follen M (2007) Real-time reflectance confocal microscopy: comparison of two-dimensional images and three-dimensional image stacks for detection of cervical precancer. J Biomed Opt 12:024021

24. Orfanoudaki IM, Themelisb GC, Sifakis SK et al (2005) A clinical study of optical biopsy of the uterine cervix using a multispectral imaging system. Gynecol Oncol 96:119–31

25. Gallwas JK, Turk L, Stepp H et al (2011) Optical coherence tomography for the diagnosis of cervical intraepithelial neoplasia. Lasers Surg Med 43:206–12

26. Ramanujam N, Mitchell MF, Mahadevan A et al (1996) Cervical precancer detection using a multivariate statistical algorithm based on laser induced fluorescence spectra at multiple excitation wavelengths. Photochem Photobiol 6:720–735

27. Arifler D, Schwarz RA, Chang SK et al (2005) Reflectance spectroscopy for diagnosis of epithelial precancer: model-based analysis

of fiber-optic probe designs to resolve spectral information from epithelium and stroma. Appl Opt 44:4291–4305

28. Marin NM, Milbourne A, Rhodes H et al (2005) Diffuse reflectance patterns in cervical spectroscopy. Gynecol Oncol 99:S116–S120

29. Kemmner W, Wan K, Rüttinger S et al (2008) Silencing of human ferrochelatase causes abundant protoporphyrin-IX accumulation in colon cancer. FASEB J 22:500–509

30. Nath A, Rivoire K, Chang S et al (2004) Effect of probe pressure on cervical fluorescence spectroscopy measurements. J Biomed Opt 9:523–33

31. Rivoire K, Nath A, Cox D et al (2004) The effects of repeated spectroscopic pressure measurements on fluorescence intensity in the cervix. Am J Obstet Gynecol 191:1606–17

32. Shim MG, Wong Kee Song LM, Marcon NE et al (2000) In vivo near-infrared Raman spectroscopy: demonstration of feasibility during clinical gastrointestinal endoscopy and para. Photochem Photobiol 72:146–150

33. Ti Y, Lin WC (2008) Effects of probe contact pressure on in vivo optical spectroscopy. Opt Express 16:4250–4262

34. Reistad N, Mayjonade M, Ahadi A et al (2015) Characterization of probe contact effects on diffuse reflectance spectroscopy measurements. Proc SPIE 9531:953143–1

35. Guido R, Schiffman M, Solomon D et al (2003) Post colposcopy management strategies for women referred with low-grade squamous intraepithelial lesions or human papillomavirus DNA-positive atypical squamous cells of undetermined significance: a two-year prospective study. Am J Obstet Gynecol 188:1401–1405

36. Mitchell MF, Schottenfeld D, Luna GT et al (1998) Colposcopy for the diagnosis of squamous intraepithelial lesions: a meta-analysis. Obstet Gynecol 91:626–631

37. Sankaranarayanan R, Gaffikinb V, Jacob M et al (2005) A critical assessment of screening methods for cervical neoplasia. Int J Gynecol Obstet 89:S4–S12

38. Mirkovic J, Lau C, Gee SM et al (2011) Detecting high-grade squamous intraepithelial lesions in the cervix with quantitative spectroscopy and per-patient normalization. Biomed Opt Express 2:2917–2925